ADM-WENO scheme and its application in compressible mixing flows

Haidong Li and Weng Kong Chan
School of MPE, Nanyang Technological University, Singapore

Received June 1998
Revised December 1998
Accepted January 1999

Keywords *Flow, High order*

Abstract *High order schemes, which are widely used in DNS and LES, received increasing attention in recent years with a number of variants being developed. However most of these schemes have difficulties in achieving high order accuracy near the boundary points. In order to solve this problem, the analytical discrete method (ADM) is proposed and presented in this paper. In addition, this method is convenient to construct the higher order WENO (weighted essentially non-oscillatory) scheme. Application of the ADM-WENO scheme to shock-tube problems and compressible mixing flows has shown it is robust and accurate in both shock-capturing and complex flow structures detection.*

Introduction

High performance computing (HPC) is enhanced by modern technologies such as domain dividing, parallel computing and convergence speeding. Meanwhile, using higher order schemes is another focus of the development of HPC. The most significant advantage of using higher order schemes is that it can reduce computing cost largely in solving multi-scale and high wave number problems due to the reduction of grids. In addition, some small structures may not be correctly detected by lower order schemes even if dense grids are used.

During the past two decades, a number of higher order finite difference schemes have been developed and they can be classified into three methods. The first type is a simple extension of the traditional finite difference method. The high order formulae of the first order derivative were given by Fornberg in 1988. He has shown that it is essential to have $n + 1$ points to evaluate the first order derivative with nth order of accuracy. Hence, it is difficult to compute derivatives accurately on the boundary and near boundary points. The second method uses half points information and reconstruction of control equations to eliminate low order truncation errors. Schemes, such as Chawla's (1975) sixth order iterative central difference scheme and Simos's (1993) two step scheme belong to this method. These schemes were successfully applied on ordinary differential equations and some simple partial differential equations such as the one dimensional convection-diffusion equation. But it is impossible to be extended to Navier-Stoke's equation due to its complicity. The last method is to consider derivatives as unknown variables in the scheme construction procedure. Most modern schemes, such as the compact scheme proposed by Orszag (1974) and Lele (1992) and the super-compact scheme developed by Ma and Fu (1995), enhance the scheme's order using this method. Applications of

International Journal of Numerical Methods for Heat & Fluid Flow, Vol. 9 No. 4, 1999, pp. 461-471.

these schemes can be found in a number of recent publications, such as Halt and Agarwal (1992) and Fu and Ma (1992). The limitation of compact and super-compact schemes is that they have to use low order schemes on the boundary points to close the solution procedure. Carpenter *et al.* (1993) and Carpenter and Scherer (1995) studied this boundary treatment problem for high order compact schemes and showed that it is very difficult to keep the scheme stable when using the same order scheme on boundary points.

Higher order computational schemes are not limited to finite difference methods. The spectral method, a well developed scheme, is widely used in turbulent flow simulations with the advantage of high order accuracy and high resolution. But it has difficulties in solving problems with complex geometry and discontinuities. Although some of the newest developments, such as Shen *et al.* (1997) can be used in discontinuity detection of the nonlinear Burgers equation and the one-dimensional shock-tube problem, they are far away from transonic compressible flow simulation.

Our research interest stems from the desire to establish a simple scheme, which can determine various order derivatives with uniform accuracy within the flow domain and boundary points. The scheme must also be easily adapted in the construction of advanced flux computing schemes. In this way, we can enhance the accuracy of the flux computing schemes and thus the solution of fluid flow equations can be improved. In this paper, fundamental concepts of the ADM will be introduced in the first section. This is followed by the construction procedure of high order ADM-WENO scheme in the second section. Finally, numerical tests of one-dimensional shock-tube problems and application in compressible mixing flows are presented in section 3 to demonstrate the capability of the new scheme. Results show that the ADM-WENO scheme can detect discontinuities and complicated flow structures accurately with high resolution.

1. Fundamental concepts of the analytic discrete method

As an example to explain the basic idea of ADM, consider an ordinary differential equation, $F(x,f,f^{(1)},f^{(2)},\cdots f^{(S)})=0$ where $\{x_j\}$ denote the coordinates of mesh points, h denotes the grid length, $\{f_j\}$ are the function values on the nodes for $j=1,2\cdots N$. The ADM with arbitrary order of accuracy can be written as:

$$\begin{cases} F(x_j,f_j,f_j^{(1)},\cdots f_j^{(S)})=0 \\ \displaystyle\sum_{s=0}^{m}\sum_{k=k_1}^{k_2}(\alpha_{s,k}^{l}h^{s}f_{j+k}^{(s)})=0 \\ l=1,2\cdots m;\ j=1,2,\cdots N \end{cases} \tag{1}$$

where m is the number of auxiliary equations which is equal to the highest derivative order. The number of scheme points equals (k_2-k_1+1). And the

highest accuracy order of the equation (1) equals $(k_2 - k_1)(m+1)$. The coefficients are $\alpha_{s,k}^l$ determined by following equations from Taylor series expansion.

$$\begin{cases} \sum\limits_{k=k_1}^{k_2} \alpha_{0,k}^l = 0 \\ \sum\limits_{k=k_1}^{k_2} (k\alpha_{0,k}^l + \alpha_{1,k}^l) = 0 \\ \cdots \\ \sum\limits_{k=k_1}^{k_2} \left(\frac{k^m}{m!}\alpha_{0,k}^l + \frac{k^{m-1}}{(m-1)!}\alpha_{1,k}^l + \cdots + \alpha_{m,k}^l \right) = 0 \\ \cdots \\ \sum\limits_{k=k_1}^{k_2} \left(\frac{k^p}{p!}\alpha_{0,k}^l + \frac{k^{p-1}}{(p-1)!}\alpha_{1,k}^l + \cdots + \frac{k^{p-m}}{(p-m)!}\alpha_{m,k}^l \right) = 0 \end{cases} \tag{2}$$

Additional constraints are needed since equation (2) is a set of non-closed equations of $\alpha_{s,k}^l$. Therefore various schemes can be obtained through choosing different constraint parameters. For example, the standard compact scheme in equation (3) can be obtained if we choose $k_1 = -1$, $k_2 = 1$, $m = 2$, $\alpha_{0,0}^1 = 0$, $\alpha_{1,0}^1 = -\frac{2}{3}$, $\alpha_{2,-1}^1 = \alpha_{2,1}^1 = 0$ and $\alpha_{0,0}^2 = -2$, $\alpha_{1,-1}^2 = \alpha_{1,0}^2 = \alpha_{1,1}^2 = 0$.

$$\begin{cases} \frac{1}{2}(f_{j+1} - f_{j-1}) - \frac{1}{6}h(f_{j+1}^{(1)} + 4f_j^{(1)} + f_{j-1}^{(1)}) = 0 \\ f_{j+1} - 2f_j + f_{j-1} - \frac{1}{12}h^2(f_{j+1}^{(2)} + 10f_j^{(2)} + f_{j-1}^{(2)}) = 0 \end{cases} \tag{3}$$

However, we cannot consider boundary treatment simultaneously if we choose constraint parameters in this way. To meet stability requirements, the energy integration by parts principle suggested by Carpenter (1993, 1995) is applied here to assist the choice of constraint parameters. For completeness, we simply describe the theory as follows.

The semi-discretization system, $\frac{\partial \hat{f}}{\partial t} + \frac{a}{\Delta x}P^{-1}Q\hat{f} = 0$, satisfies the summation-by-parts energy norm and it is linearly stable if P and Q satisfy

(1) Symmetric $P : p_{ij} = p_{ji}$;

(2) Positive definite $P : W^T PW > 0$;

(3) Nearly skew-symmetric $Q : q_{ij} + q_{ji} = 2\delta_{i1}\delta_{1j} + 2\delta_{iN}\delta_{Nj}$;

(4) $q_{NN} = -q_{11} = \frac{1}{2}$.

In fact, the product of matrix P and Q is the first order derivative calculation matrix. Thus the construction of the ADM scheme is changed to determine matrices P and Q through solving those coefficients in equation (2) according to the above principle. In this paper, we illustrate the third order and fifth order schemes while other order schemes can be found in Li (1997).

In the third order scheme,

$$P_3 = \begin{bmatrix} 1/4 & 1/8 & 0 & 0 \\ 1/8 & 5/4 & -1/4 & 0 \\ 0 & -1/4 & 5/4 & 1/8 \\ 0 & 0 & 1/8 & 1/4 \end{bmatrix}, \quad Q_3 = \begin{bmatrix} -1/2 & 11/16 & -1/4 & 1/16 \\ -11/16 & 0 & 15/16 & -1/4 \\ 1/4 & -15/16 & 0 & 11/16 \\ -1/16 & 1/4 & -11/16 & 1/2 \end{bmatrix}$$

And in the fifth order scheme,

$$P_5 = \begin{bmatrix} 1 & \frac{28}{31} & -\frac{25}{93} & 0 & 0 & 0 \\ \frac{28}{31} & \frac{2251}{279} & -\frac{506}{93} & \frac{395}{93} & -\frac{370}{279} & 0 \\ -\frac{25}{93} & -\frac{506}{93} & \frac{514}{31} & -\frac{1006}{93} & \frac{395}{93} & 0 \\ 0 & \frac{395}{93} & -\frac{1006}{93} & \frac{514}{31} & -\frac{506}{93} & -\frac{25}{93} \\ 0 & -\frac{370}{279} & \frac{395}{93} & -\frac{506}{93} & \frac{2251}{279} & \frac{28}{31} \\ 0 & 0 & 0 & -\frac{25}{93} & \frac{28}{31} & 1 \end{bmatrix},$$

$$Q_5 = \begin{bmatrix} -\frac{384}{155} & \frac{773}{186} & -\frac{866}{279} & \frac{67}{31} & -\frac{82}{93} & \frac{407}{2790} \\ -\frac{773}{186} & 0 & \frac{731}{93} & -\frac{598}{93} & \frac{671}{186} & -\frac{82}{93} \\ \frac{866}{279} & -\frac{731}{93} & 0 & \frac{2518}{279} & -\frac{598}{93} & \frac{67}{31} \\ -\frac{67}{31} & \frac{598}{93} & -\frac{2518}{279} & 0 & \frac{731}{93} & -\frac{866}{279} \\ \frac{82}{93} & -\frac{671}{186} & \frac{598}{93} & -\frac{731}{93} & 0 & \frac{773}{186} \\ -\frac{407}{2790} & \frac{82}{93} & -\frac{67}{31} & \frac{866}{279} & -\frac{773}{186} & \frac{384}{155} \end{bmatrix}$$

We observe that it still has the limitation at nth order scheme needs $(n+1)$ points. However, now not only the calculation procedure is simplified to a narrow bandwidth matrix operation, but also it can deal with boundary points without any difficulty. The higher order derivatives can also be evaluated by repeating the same matrix operation. For example,

$$\begin{aligned} \left\{f^{(1)}\right\} &= P^{-1}Q\{f\} \\ \left\{f^{(2)}\right\} &= P^{-1}Q\left\{f^{(1)}\right\} \end{aligned} \tag{4}$$

2. Construction procedure of ADM-WENO scheme

The WENO scheme developed by Liu (1994) is a modified version of ENO schemes. Compared to the traditional ENO schemes proposed by Harten (1989), there is no need to choose the smoothest stencil to construct the interpolating polynomial in the ENO flux reconstruction procedure. Since it considers all the candidates to achieve the essentially non-oscillatory property, the computational efficiency can be improved greatly. Unfortunately, it has the same problem with boundary treatment because more computing points will be

involved when we increase the accuracy order. Here we reformed the numerical fluxed calculation with ADM formulae so that it can keep the original accuracy order on boundary points.

The rth order ADM-WENO flux of scale equation $\frac{\partial u}{\partial t}+\frac{\partial f}{\partial x}=0$ can be written as:

$$\begin{aligned}\tilde{f}^{+}_{j+1/2} &= \sum_{s=-1}^{1} W_s p_{j+s}(x_{j+1/2}) \\ p_{j+s}(x) &= \sum_{k=0}^{r-1}\frac{1}{k!}\left(\frac{\partial^k f}{\partial x^k}\right)_{j+s}(x-x_{j+s})^k \\ &+ \sum_{k=1}^{(r-1)/2} C_{2k}\left(\frac{\partial^{2k} f}{\partial x^{2k}}\right)_{j+s}(x-x_{j+s})^{2k}+O(h^{r+1}) \\ & s=-1,\ 0,\ 1\end{aligned} \tag{5}$$

Where C_{2k} are ENO correcting coefficients determined by the following equations.

$$\begin{cases}\frac{1}{2^2\cdot 3!}+\frac{C_2}{2^0\cdot 1!}=0 \\ \frac{1}{2^4\cdot 5!}+\frac{C_2}{2^2\cdot 3!}+\frac{C_4}{2^0\cdot 1!}=0 \\ \frac{1}{2^6\cdot 7!}+\frac{C_2}{2^4\cdot 5!}+\frac{C_4}{2^2\cdot 3!}+\frac{C_6}{2^0\cdot 1!}=0 \\ \cdots \\ \frac{1}{2^{2c}\cdot(2c+1)!}+\frac{C_2}{2^{2(c-1)}\cdot(2c-1)!}+\cdots+\frac{C_{2c-2}}{2^2\cdot 3!}+\frac{C_{2c}}{2^0\cdot 1!}=0\end{cases} \tag{6}$$

The first three items can be found easily, $C_2=-\frac{1}{24}$, $C_4=\frac{7}{5760}$ and $C_6=-\frac{31}{967680}$. $W_s=\frac{\beta_s}{(\varepsilon+IS_s)^q}$ is weight factor. Parameter β_s and q are chosen as $\beta_{-1}=\frac{1}{10}$, $\beta_0=\frac{6}{10}$, $\beta_1=\frac{3}{10}$ and $q=2$ according to Liu *et al.* (1994). IS_s is the smoothness indicator of the sth interpolation polynomial, which is defined as:

$$IS_s=\sum_{l=1}^{r-1}\int_{j-1/2}^{j+1/2}(p^{(l)}_{j+s}(x))^2 h^{2l-1}\cdot dx,\quad s=-1,\ 0,\ 1; \tag{7}$$

Substituting equation (5) into (7), and choosing , we obtain

$$\begin{cases} IS_{-1}=\frac{13}{12}h^4(f^{(2)}_{j-1})^2+(h^2 f^{(2)}_{j-1}+h f^{(1)}_{j-1})^2 \\ IS_0=\frac{13}{12}h^4(f^{(2)}_{j})^2+(h f^{(1)}_{j})^2 \\ IS_1=\frac{13}{12}h^4(f^{(2)}_{j+1})^2+(h^2 f^{(2)}_{j+1}-h f^{(1)}_{j+1})^2\end{cases} \tag{8}$$

$f^{(1)}_{j+s}$ and $f^{(2)}_{j+s}$ will be calculated using ADM formulae described in the above section. The negative flux $\tilde{f}^{-}_{j-1/2}$ can be constructed in the same way as long as we substitute $x_{j-1/2}$ instead of $x_{j+1/2}$ in equation (5).

When we apply these formulae to the Navier-Stoke's equation, characteristic projection is needed to eliminate non-physical oscillations. That means all the f in equation (4) to (8) should be changed to characteristic variables $f_c = L \cdot f$, and after reconstruction, the numerical fluxes in the characteristic field have to be inversely projected to the physical domain by $f = f_c \cdot R.L$ and R can be evaluated from the Jacobian matrix $A = \frac{\partial f}{\partial U} = L\Lambda R$.

3. Numerical experiments

In order to demonstrate the validity and capability of the present scheme, two one-dimensional shock-tube problems are chosen as test examples.

3.1 Shock-tube 1

We consider the following Riemann problem

$$U_0(x) = \begin{cases} U_L\ , & x < 0 \\ U_R\ , & x > 0 \end{cases}, U = (\rho, \rho u, \rho e) \tag{9}$$

Here $U_L = (1., 0., 1.)$ and $U_R = (0.125, 0., 0.1)$. We test our scheme with $r = 3$. Figure 1 shows the curves of pressure, velocity and density distribution in the tube. We observed that the numerical solution is smooth in the discontinuous area with high resolution. The shock wave can be accurately captured by 1 grid

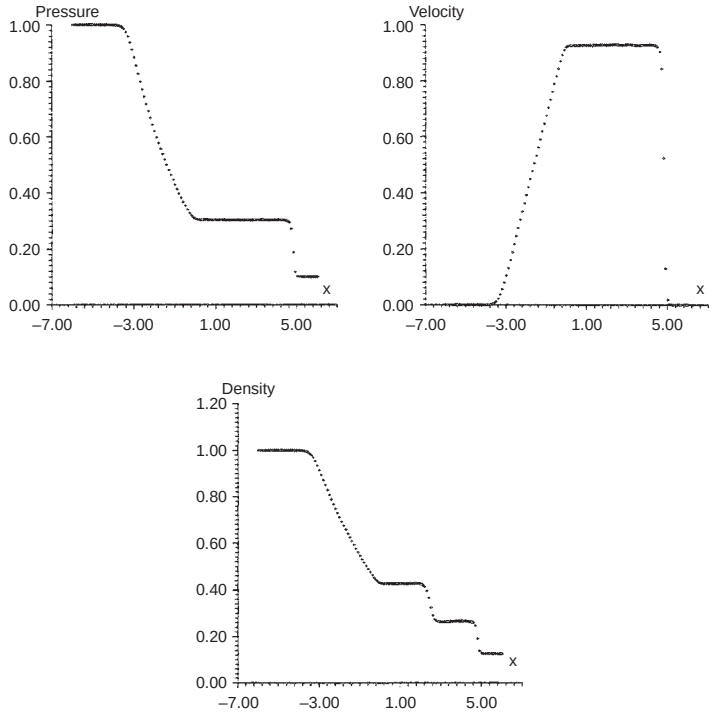

Figure 1.
Pressure, velocity and density distribution of shock-tube 1

cell. This result is much better than the result of the second order TVD scheme developed by Wu (1989), and the ADM-ROE scheme developed by Li *et al.* (1996).

3.2 Shock-tube 2

It is a similar problem as 3.1, but with different initial boundary conditions.

$$\begin{cases} \rho_L = 3.857, u_L = 2.629, p_L = 10.333; \ x < -4 \\ \rho_R = 1 + 0.2\sin(5x), u_R = 0, p_R = 1; \ x \geq -4 \end{cases} \tag{10}$$

Although this example cannot be solved analytically, it is a typical test problem of high order schemes because the wave shape is closely related to the diffusion characteristics of various schemes. As shown in Figure 2, the numerical results of present scheme at $t = 1.8s$ is identical with those of other higher order schemes such as Huynh's scheme (1995) and the time-space conservative scheme by Wang and Chow (1996).

3.3 2D mixing flow

The investigation of compressible mixing flows was motivated by the development of ramjet because combustion efficiency is largely dependent on the mixing level of fuel and oxygen. Compressibility can have strong effects on

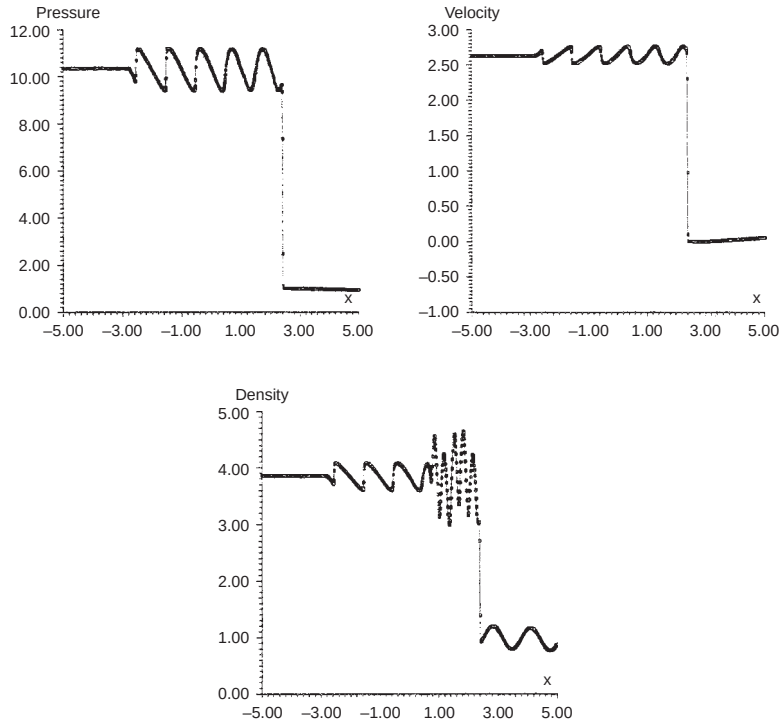

Figure 2.
Pressure, velocity and density distribution of shock-tube 2

the development of mixing layers, see Sandham (1994) and Soetrisno *et al.* (1989). The most well known feature of the compressible mixing layer is the reduction in growth rate. In this paper, investigations are made into the mechanisms affecting the vortex pairing process.

The simulations are made for a temporally evolving mixing layer with equal and opposite free stream velocities and equal free stream densities. The nondimensionalized initial velocity profile is given by $\bar{u} = \tanh(2y)$, and initial temperature is given according to the Crocco-Busemann relation

$$\bar{T} = 1 + \frac{\gamma - 1}{2} M_c^2 (1 - \bar{u}^2) \tag{11}$$

Here M_c is the convection Mach number of the flow. For this case $M_c = {}^{U_1}/_{a}$, where U_1 is the free stream velocity and a is the free stream sound speed. Pressure is assumed to be uniform at the inlet. Nondimensional dynamic viscosity is set to $\mu = T^{2/3}$ and Reynolds number is set to 2000 based on the inlet velocity and length of the computational domain. To force the pairing process, disturbances consisting of a fundamental and a sub-harmonic wave are added to the initial mean velocity profiles as follows.

$$\begin{aligned} u' &= -A_1 \frac{yL_x}{2\pi B} \cos\left(\frac{4\pi x}{L_x}\right) \exp\left(\frac{-y^2}{B}\right) - A_2 \frac{yL_x}{\pi B} \cos\left(\frac{2\pi x}{L_x}\right) \exp\left(\frac{-y^2}{B}\right) \\ v' &= A_1 \sin\left(\frac{4\pi x}{L_x}\right) \exp\left(\frac{-y^2}{B}\right) + A_2 \sin\left(\frac{2\pi x}{L_x}\right) \exp\left(\frac{-y^2}{B}\right) \end{aligned} \tag{12}$$

This provides a standard divergence-free disturbance to the mixing layer with a phase of zero between the fundamental and sub-harmonic wave. And the pairing is excited most efficiently due to this disturbance. The amplitudes are

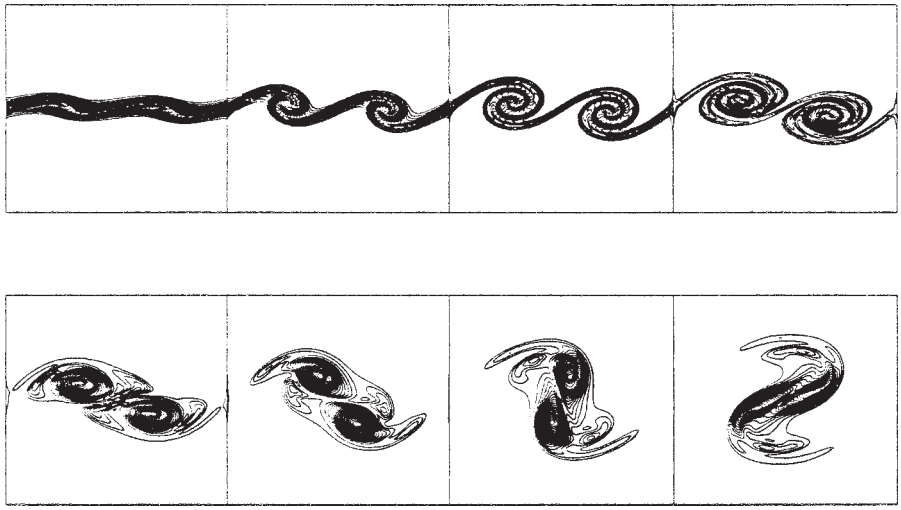

Figure 3.
Vorticity contours of Mc = 0.2

chosen to be $A_1 = 0.05$ and $A_2 = 0.025$. The parameter B was set to ten. Length of the computational domain is specified as $L_x = 20$ and $L_y = 20$. Grid size of 129×101 and third order ADM-WENO scheme are used in the simulation. Figures 3, 4 and 5 show the overall shear layer evolution procedure with different Mach numbers. Figure 6 shows the comparison of vorticity thickness (defined as $\delta = \frac{U_1 - U_2}{(\partial u / \partial y)_{\max}}$) development history of different

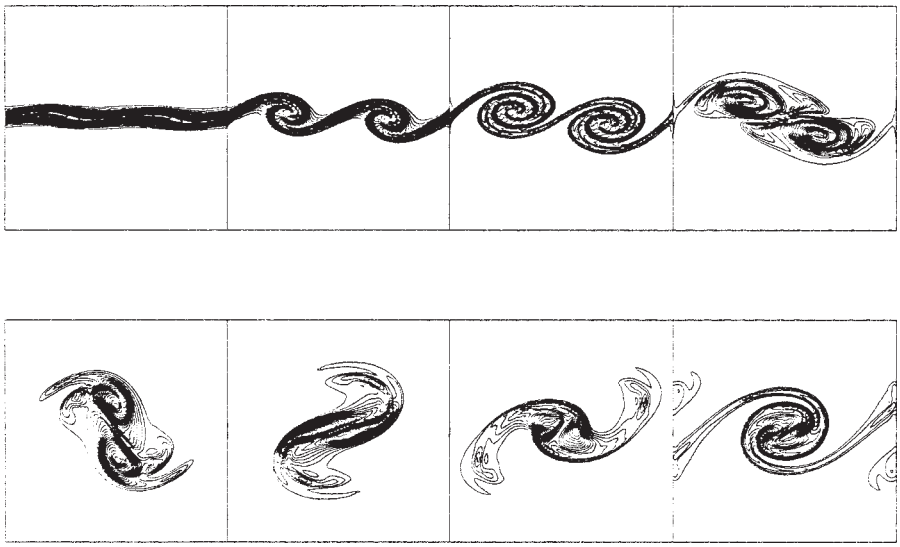

Figure 4.
Vorticity contours of Mc = 0.4

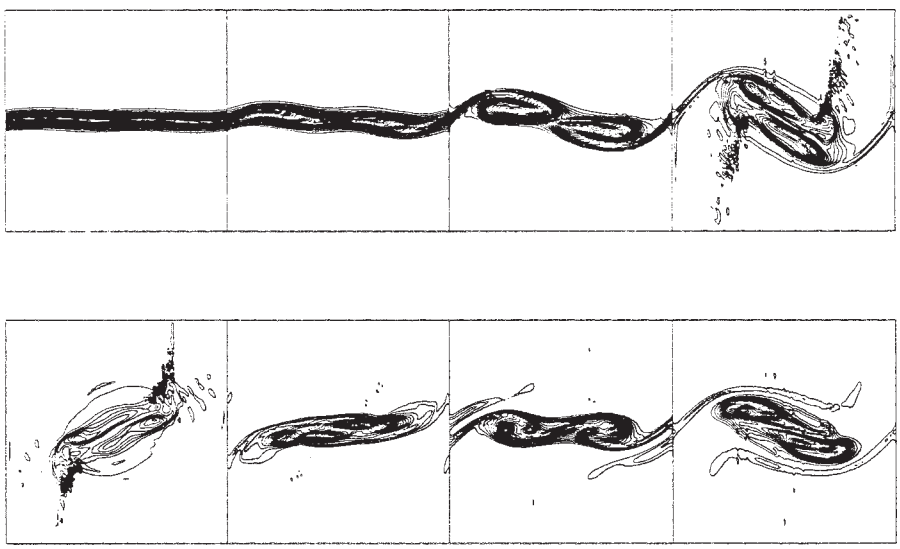

Figure 5.
Vorticity contours of Mc = 0.8

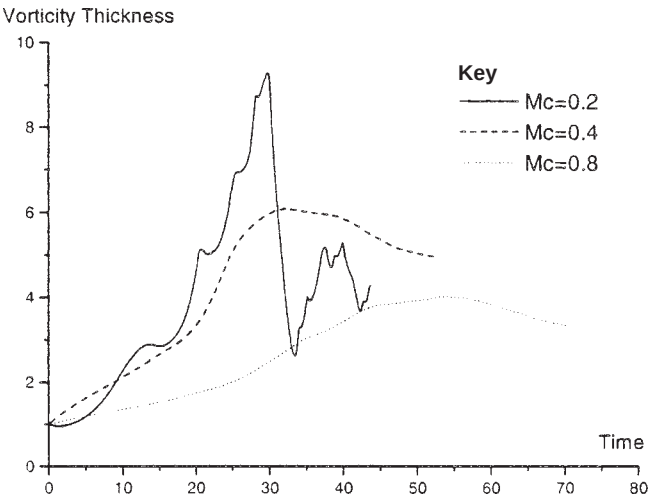

Figure 6.
Vorticity thickness development history

convection March number. We observe that not only the mixing layer growth rate is strongly affected by the Mach number, but also the shape and the rotating speed of vortex pairs are different. In the case of $M_c = 0.8$, vortexes are broken and shock waves appear when $t > 125$. It coincides with the common knowledge that shock waves may appear when $M_c > 0.75$.

4. Conclusion remarks

A numerical method (ADM) of derivative calculation with consideration of boundary treatment has been developed. At mean time, three examples of ADM and the construction procedure of ADM-WENO scheme are presented in this paper. Reasonable results from numerical tests and compressible mixing layer simulations have shown that the ADM-WENO scheme is an accurate scheme for compressible flow simulation with high resolution.

References

Carpenter, M.H. and Scherer, G. (1995), "High-order 'cyclo-difference' techniques: an alternative to finite differences", *J. of Comput. Phys.*, Vol. 118, pp. 242-60.

Carpenter, M.H., Gottlieb, D. and Abarbanel, S., (1993), "Stable and accurate boundary treatments for compact, high-order finite-difference schemes", *Appl. Numer. Math.*, Vol. 12, pp. 55-87.

Chawla, M.M. (1975), "A sixth order tridiagonal finite difference method for non-linear two-point boundary value problems", BIT 17, pp. 128-33.

Fornberg, B. (1988), "Generation of finite difference formula on arbitrary spaced grids", *Math. of Comp.*, Vol. 51 No. 184, pp. 699-706.

Fu, D.X. and Ma, Y.W. (1992), "Numerical simulation of physical problems with high order finite difference schemes", *Chinese J. of Comp. Phys.*, Vol. 9 No. 4, pp. 501-5.

Halt, D.W. and Agarwal, R.K. (1992), "Compact high order characteristic-based Euler solver for unstructured grids", *AIAA J.*, Vol. 30 No. 8, pp. 1993-9.

Harten, A. (1989), "ENO scheme with subcell resolution", *J. of Comput. Phys.*, Vol. 83, pp. 148-84.

Huynh, H.T. (1995), "Accurate upwind schemes for the Euler equations", AIAA Paper: 95-1737-CP

Lele, S.K. (1992), "Compact finite difference schemes with spectral-like resolution", *J. of Comput. Phys.*, Vol. 103, pp. 16-42.

Li, H.D. (1997), "High order analytic discretization method and its application", PhD thesis, Tsinghua University.

Li, H.D., Liu, Q.S. and Shen, M.Y. (1996), "High order accuracy scheme for 2-D transonic cascade flows", *Chinese J. of Aeronautics*, Vol. 9 No. 2, pp. 86-91.

Liu, X.D., Osher, S. and Chan, T. (1994), "Weighted essentially non-oscillatory schemes", *J. of Comput. Phys.*, Vol. 115, pp. 200-12.

Ma, Y.W. and Fu, D.X. (1995), "Super compact finite difference method with uniform and nonuniform grid system", *Sixth Inter. Symp. on CFD*, Nevada, USA, pp. 1435-9.

Orszag, S.A. and Israeli, M. (1974), "Numerical simulation of viscous incompressible flows", Flow Research Report No. 17, Flow Research Inc., Kent Wash.

Sandham, N.D. (1994), "The effect of compressibility on vortex pairing", *Phys. Fluids*, Vol. 6 No. 2, pp. 1063-72.

Shen, M.Y., Zhang, Z.C. and Li, H.D. (1997), "New high accuracy three-point finite spectral scheme", *J. of Tsinghua University (Sci & Tech)*, Vol. 37 No. 8, pp. 52-4.

Simos, T.E. (1993), "High order methods with minimal phase-lag for the numerical integration of the special second-order IVP and their application on the 1D Schroodinger equation", *Comp. Phys. Commun.*, Vol. 74, pp. 63-6.

Soetrisno, M. *et al.* (1989), "A study of inviscid supersonic mixing layer using second order TVD scheme", *AIAA J.*, Vol. 27 No. 12, pp. 1770-8.

Wang, X.Y. and Chow C.Y. (1996), "High resolution element method", AIAA Paper:-0764.

Wu, H.M. (1989), "New accurate high resolution TVD schemes – analysis and applications", *Inter. Symp. on CFD*, Nagoya, Japan.